

Dipolar ordering and glassy freezing in a clathrate

This article has been downloaded from IOPscience. Please scroll down to see the full text article.

2000 Europhys. Lett. 51 407

(<http://iopscience.iop.org/0295-5075/51/4/407>)

View [the table of contents for this issue](#), or go to the [journal homepage](#) for more

Download details:

IP Address: 130.113.174.172

The article was downloaded on 04/07/2012 at 19:14

Please note that [terms and conditions apply](#).

Dipolar ordering and glassy freezing in a clathrate

H. WOLL, M. ENDERLE, A. KLÖPPERPIEPER, M. C. RHEINSTÄDTER,
K. KIEFER, F. KRUCHTEN and K. KNORR

Technische Physik, Universität des Saarlandes - 66041 Saarbrücken, Germany

(received 25 February 2000; accepted 8 June 2000)

PACS. 64.60.Cn – Order-disorder transformations; statistical mechanics of model systems.

PACS. 64.70.Pf – Glass transitions.

PACS. 77.22.Ch – Permittivity (dielectric function).

Abstract. – The dielectric permittivity of methanol- β -quinol clathrates has been studied as a function of temperature, frequency and methanol concentration. Higher concentrated samples undergo a first-order antiferroelectric transition, lower concentrated ones are established as dipole glasses. The main structural motif are ferroelectric chains, respectively chain segments. The largely different strength of the intrachain and the interchain coupling, the frustration leading to the glass state, and the relaxational dynamics are interpreted in terms of the dipole-dipole interaction in combination with the rhombohedral symmetry of the host lattice.

Glassy disorder and freezing is a major challenge to condensed matter physics. The dipole glasses [1], mixed crystals in which electric dipole moments freeze into a state without long-range order, are hoped to mediate between the real glasses and the disordered magnetic systems called spin glasses [2]. Indeed the dipole glasses share the complex distribution of relaxation times [3–7] and the fact that freezing involves atomic positions with the real glasses. On the other hand, both the dipole and the spin glasses rely on the quenched substitutional disorder of a mixed crystal and it is suggestive to consider the orientational degrees of freedom of the electric and magnetic dipole moments equivalent. Nevertheless the application of the well-established spin glass models to dipole glasses is problematic. What is the reason? Popular examples of dipole glasses are $\text{Rb}_{1-x}(\text{NH}_4)_x\text{H}_2\text{PO}_4$ [3], a member of the KDP family, and cubic perovskites, such as $\text{K}_{1-x}\text{Li}_x\text{TaO}_3$ [4]. The dipole moments originate from the displacements of the protons along the $\text{O}-\text{H}\cdots\text{O}$ bonds and from the off-center position of the Li-ion, respectively. However, these atoms also participate in the bonding of the crystal. Therefore the distinction between the elementary dipole moments and a background lattice is difficult. The bare moments resulting from the displacement of these atoms are dressed by polarization and strain clouds of the lattice and the interaction between the effective moments is rather complex due to lattice-mediated contributions. This is presumably the major reason why studies on dipole glasses usually concentrate on the phenomenology of the glassy relaxations rather than on the microscopic interactions.

An electric-dipole glass suitable for a microscopic description in terms of spin glass models [2] should consist of well-defined dipoles which occupy the nodes of a rigid lattice statistically and are coupled by a well-defined interaction. We will establish the methanol- β -

TABLE I – The phase transition temperature T_s , the intrachain J_c and the interchain J_\perp coupling parameter, and the Arrhenius barrier E_A (all in units of K) as a function of the methanol occupancy x .

x	0.97(± 0.02)	0.84	0.79	0.73	0.50	0.40
T_s	63.9(± 0.1)	50.3	45.2	–	–	–
J_c	195(± 5)	175	176	155	121	111
J_\perp	-0.3(± 0.2)	-1.6	-2.2	-3.2	-6.1	-7.5
E_A	848(± 15)	833	830	831	820	815

hydroquinon clathrate as a dipole glass which gets close to this situation. Accordingly the emphasis of our work is on the interactions, but we will also give some comments on the relaxations.

In the β -modification the quinol (HO-C₆H₄-OH) molecules form a H-bonded rhombohedral R $\bar{3}$ lattice with about spherical cavities, one per unit cell [8]. The methanol guest molecules residing in these cavities are bound to the quinol host lattice by weak dispersion forces only. Therefore, they can reorient relatively freely and the dipole moment is that of the free molecule ($\mu = 1.69D$). From the local C_{3i} symmetry of the cavity center one expects a set of 6 equivalent orientations [9] of the dipole moment. At 65 K the methanol clathrate shows a phase transition in which the dipole moments order collectively [10, 11]. Similar phase transitions have been observed for other dipolar guest molecules. The transition temperatures T_s were found to scale with μ^2 [12], suggesting that the dominant coupling between the guest molecules is the electrostatic dipole-dipole (EDD) interaction. The host lattice tolerates methanol concentrations x as low as 0.35 without collapsing. Thus the effect of random site occupation on electric ordering and glassy freezing and the crossover between these two cases can be studied. We have investigated a series of six single crystals with different methanol concentrations (see table I).

The three higher concentrated samples, $x > x_c$, show conventional ordering via a first-order phase transition, whereas the others, $x < x_c$, freeze into dipole glasses, $x_c \cong 0.76$. The complex dielectric permittivity $\varepsilon(T, f)$ has been measured with the electric field applied parallel (ε_c) and perpendicular (ε_a) to the threefold symmetry axis. The measuring frequencies f span a range from 100 Hz to 1 MHz for the higher and from 0.01 Hz to 1 MHz for the lower concentrated samples. Figures 1 and 2 show such data on ε_c for the samples with the highest and the lowest concentration.

In contrast to ε_c , ε_a is weakly temperature dependent only, with maximum values (varying between 5 and 5.5 for the different samples) being only slightly larger than ε_∞ (between 3.8 and 4.2). Our complementary X-ray diffraction experiments show that the low- T phase of the $x = 0.97$ sample is not R3 ferroelectric, as stated previously [11], but rather antiferroelectric triclinic without a global threefold symmetry and accordingly with three orientation states. The structure basically consists of ferroelectric chains running along c which are arranged in sheets of alternating sign, as evidenced by superlattice reflections and presumed previously [13]. The dielectric data of all samples show primary relaxations in ε_c at temperatures comparable to the transition temperatures of the ordering samples and secondary relaxations in ε_a at lower T around 20 K. ε_c is significantly larger than ε_a , indicating that it is mainly the c -component of μ , μ_c , which is involved in the primary relaxations and the ordering process, whereas the perpendicular component is involved in the secondary relaxations. Figure 3 shows the temperature dependence of the static permittivity ε_{cs} along c .

In the regime of dispersion, values of ε_{cs} have been obtained at discrete temperatures from

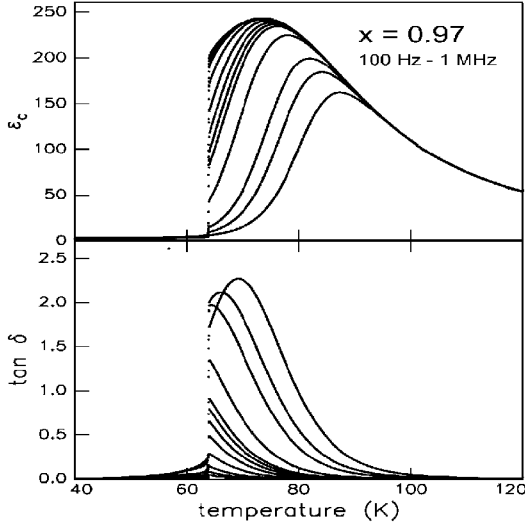


Fig. 1

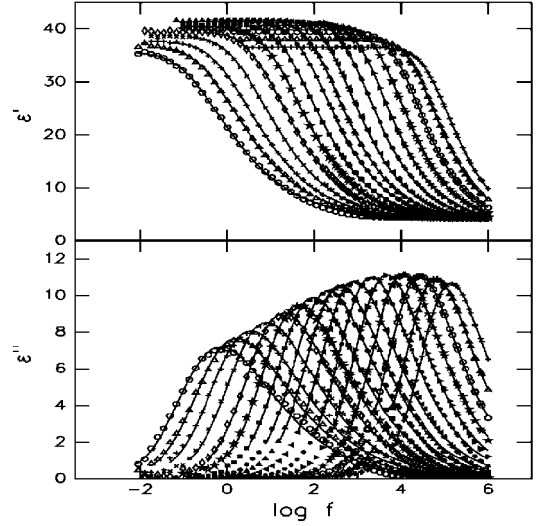


Fig. 2

Fig. 1 – The permittivity along c and the loss angle for $x = 0.97$ as a function of temperature for a series of measuring frequencies.

Fig. 2 – The real ε' and imaginary ε'' part of the permittivity along c for $x = 0.40$ as a function of the measuring frequency f and the temperature as parameter. The temperatures range from 31.7 K (left) to 58.4 K (right) in steps which are equidistant on a $1/T$ -scale. Solid lines are fits of the KWW relaxation law.

the analysis of the f -dependence in terms of the relaxation models of Havriliak-Negami and Kohlrausch-Williams-Watts (KWW). ε_{cs} shows strong deviations from the Curie-Weiss law already at 250 K. The behavior of $\varepsilon_{cs}(T)$ at higher T is well described by the susceptibility of the one-dimensional (1D) Ising model with a coupling J_c to the next neighbors within the chains and an interchain interaction J_{\perp} which is treated in mean-field approximation [14]. The fit of the model to the data (fig. 3) yields the intra- and the inter-chain coupling constants (see table I). The values of J_c and J_{\perp} for $x = 0.97$ are in reasonable agreement with calculations of the EDD interaction for fully occupied chains. At lower T , $\varepsilon_{cs}(T)$ deviates from the Ising-behavior and finally decreases with decreasing T , indicating the onset of 3D antiferroelectric interchain correlations. For the higher concentrated samples, these correlations eventually lead to the antiferroelectric phase transition at T_s , where both ε_c and ε_a drop to lower values. The drop is rather sharp not only for the practically fully concentrated $x = 0.97$ sample but also for $x = 0.84$ and 0.79 . This means that the transition is not smeared out by a variation of the methanol concentration across the samples, but that the methanol molecules occupy the lattice sites statistically.

For $x = 0.97$, J_{\perp} is about three orders of magnitude smaller than J_c . This extremely 1D behavior is not so much due to largely different distances d [8] of intrachain neighbors (two at $d_1 = c = 5.6 \text{ \AA}$) and interchain neighbors (six at $d_2 = 9.6 \text{ \AA}$ and six at $d_{2'} = 10.1 \text{ \AA}$), but is a peculiarity of the EDD interaction in combination with the lattice symmetry. The ferroelectric interactions along the chain add up, while the interactions to adjacent chains cancel each other almost perfectly due to the triangular symmetry. The already small remainder of the antiferroelectric interchain interaction decreases with the increasing ferroelectric correlation

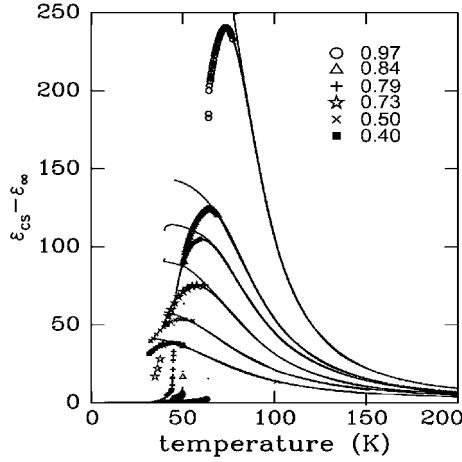


Fig. 3 – The static permittivity $\varepsilon_{CS} - \varepsilon_{\infty}$ along c as a function of T for all samples investigated. The discrete data points of the dispersion regime have been derived from the analysis of relaxational models, the data points at higher temperatures form quasicontinuous curves which coincide almost perfectly with fits based on the quasi-1D Ising model.

along the chains. The correlation length along the chains x can be estimated from J_c , $(\xi/c)^2 = 0.25 \exp[4J_c/T]$, thus ξ increases on cooling, reaching values of some hundreds in units of c before eventually the 3D antiferroelectric correlations develop. The weak interchain coupling enhanced by a high 1D order along the chains shifts the phase transition of isolated chains from $T = 0$ to a 3D ordering temperature T_s which is much higher than J_{\perp} , $T_s = |J_{\perp}| \exp[2J_c/T_s]$. With decreasing occupancy x , T_s shifts to lower T more quickly than expected for the mean-field case $T_s(x) = xT_s(x = 1)$.

For $x < 0.79$, the phase transition is no longer observed. Even down to the lowest x investigated, the 1D Ising model with a coupling to the next neighbors of a fully occupied chain combined with mean-field interchain interactions supplies an excellent description of the permittivity data at higher T . In fact, the extension of this model to chains with a small percentage of vacancies [15] cannot describe the data. The effective intrachain interaction J_c decreases with x , but not as fast as $xJ_c(x = 1)$. We attribute this to the long (but not infinite) range of the EDD interaction. Obviously the ferroelectric correlations are not cut off by an empty cavity, which would be the case if the intrachain coupling were restricted to first neighbors [15]. Surprisingly enough, the interchain interaction J_{\perp} on the other hand increases significantly with decreasing occupancy. In the fully occupied system the main part of the interchain interaction was cancelled by the threefold symmetry. If this compensation is destroyed by empty cavities, the effective, mean-field interchain interaction J_{\perp} becomes larger. It also becomes larger with decreasing ferroelectric correlation along the chains due to the dipolar nature of the interaction. J_{\perp} is however still very much smaller than the intrachain coupling J_c . Hence the increase of J_{\perp} with decreasing occupancy cannot compensate the decrease of J_c , with the consequence that eventually 3D ordering is suppressed. We imagine the partially occupied system as consisting of chain segments of ferroelectrically correlated dipoles. The interchain interaction is then always of the antiferroelectric type, but its strength and the preference direction of the dipoles depend on the length of the segments and relative position of these segments on the chains. This must lead to significant frustration in a rhombohedral lattice. While T_s of the long-range ordered system is given by the Fourier transform of the

interactions at the ordering wave vector, a glass transition is expected at a temperature T_g which corresponds to the mean interaction per bond. Because of the compensation of the interchain interactions in the ordered phase, T_g for x slightly below x_c could be even higher than T_s for x slightly above x_c .

The frequency dependence of the complex permittivity has been analyzed. We refer to the results obtained with the KWW model, which is the model with the smallest number of free parameters, namely the average relaxation time τ and the stretching exponent α . Fits of this model to the ε'_c and ε''_c data are nevertheless of excellent quality. See fig. 2 for $x = 0.40$. Results on $\tau(T)$ and $\alpha(T)$ are of course only available in the T -range in which $1/\tau$ is comparable to the measuring frequency f . For the almost fully occupied sample, $x = 0.97$, the relaxations of the paraelectric phase are close to the Debye case with a narrow τ -distribution. α decreases with decreasing T and with decreasing x without any apparent change of the behavior at x_c . For the samples with $x < x_c$, for which the relaxational behavior is not interrupted by the phase transition, data are available down to about 30 K. Here $\alpha \approx 0.5$, which is indicative of the broad τ -distribution which—in combination with the absence of long-range ordering—is usually regarded as the main piece of evidence for glassy freezing. For $x = 0.40$, the large width of the τ -distribution at lower T is also directly apparent from fig. 2. The T -dependence of τ follows the Arrhenius law, $1/\tau = f_0 \exp[-E_A/T]$ rather than the Vogel-Fulcher law $1/\tau = f_0 \exp[-E_A/(T - T_{vf})]$. The values for the energy barrier E_A are included in the table, the values of the attempt frequency f_0 are around 20 GHz. Arrhenius laws with similar values of E_A and f_0 are also obtained for the loci of f, T -combinations taken at different relative heights δ of the dispersion step of ε'_c . This method, the so-called δ -plot, probes a weighed τ -distribution, the weight of the slow relaxations increases with increasing δ [3]. Other dipole glasses [3–7] have τ -distributions of similar width but there are examples [6, 7] for which the Arrhenius law for the average relaxation time changes over to the Vogel-Fulcher law in the long- τ tail of the distribution. The present results suggest that all parts of the relaxation spectrum obey the Arrhenius law.

The knowledge of the coupling parameters allows an insight into the origin of the relaxations. The dynamics of the 1D Ising chain [16] and of the quasi-1D Ising system with mean-field interchain coupling [17] have been described in the literature. Because of the smallness of J_\perp , we can safely refer to the pure 1D case [16]. For $J_c/T > 1$ the relaxation time is given approximately by $\tau = \tau_{loc} \exp[4J_c/T]$. Here τ_{loc} is the relaxation time of an individual dipole in the thermal bath decoupled from the other dipoles. We think of these relaxations in terms of flips of μ_c in the crystal field of the cavity, the relaxation time being given by $\tau_{loc} = \tau_{0,loc} \exp[E_{loc}/T]$, where E_{loc} is the barrier for such flips. Hence the effective barrier E_A from above decomposes into $E_A \approx E_{loc} + 4J_c$. The values of E_A and J_c (see table I) suggest that for $x = 0.97$, E_A is mainly due to the dipolar coupling J_c , leaving only about 70 K for the local crystal field barrier E_{loc} . The height of the local barrier increases with decreasing occupancy. For $x = 0.40$, E_{loc} is about 370 K and supplies about one half of the total barrier. Obviously the cavities are distorted by vacancies in neighboring cavities. Such effects have to be classified as fields, as random fields since they depend on the occupation statistics, a quenched variable, rather than on the orientations of the neighboring dipoles. In this sense the freezing of the low-concentrated samples is about half way between a local freezing in random fields and collective spin-glass-like freezing due to random interactions. The freezing of the glassy sample with $x = 0.73$ is however dominated by random interactions ($E_{loc} \approx 210$ K, $4J_c \approx 620$ K) and should be therefore close to spin-glass-like.

In summary, we have shown that the long-range dipolar ordering of the β -quinol methanol clathrates, the size of the interactions and their change with the occupancy as well as the relaxational dynamics which at lower occupancies lead to glass-like low- T state can be explained

by the peculiar properties of the dipole-dipole interaction in this rhombohedral lattice. The clathrates would be highly suited for computer simulations, which could start almost from first principles. Thus the clathrates could contribute to a microscopic understanding of the dipole glass state on a level comparable to what has been achieved in the best examples of spin glass systems. They may also contribute to the understanding of disordered dipolar magnetic system [18] such as frozen ferrofluids.

* * *

This work has been supported by the Deutsche Forschungsgemeinschaft. The dielectric measurements at lower frequencies have been carried out at the university of Augsburg. We thank the group of Prof. A. LOIDL for hospitality and assistance. We are grateful to W. KOB for helpful discussions.

REFERENCES

- [1] HÖCHLI U. T., KNORR K. and LOIDL A., *Adv. Phys.*, **39** (1990) 405.
- [2] BINDER K. and YOUNG A. P., *Rev. Mod. Phys.*, **58** (1986) 801.
- [3] KUTNJAK Z., FILIPIC C., LEVSTIK A. and PIRC R., *Phys. Rev. Lett.*, **25** (1993) 4015.
- [4] KLEEMANN W. and KLÖSSNER A., *Europhys. Lett.*, **35** (1996) 391.
- [5] WINTERLICH M., BÖHMER R. and LOIDL A., *Adv. Phys.*, **75** (1995) 1783.
- [6] KUTNJAK Z., PIRC R., LEVSTIK A., FILIPIC I., FILIPIC C., BLINC R. and KIND R., *Adv. Phys.*, **50** (1994) 12421.
- [7] HEMBERGER J., RIES H., LOIDL A. and BÖHMER R., *Adv. Phys.*, **76** (1996) 2330.
- [8] PARSONAGE N. G. and STAVELEY L. A. K., in *Disorder in Crystals* (Clarendon Press, Oxford) 1978, Chapt. 11.
- [9] RIPMEESTER J. A., HAWKINS R. E. and DAVIDSON D. W., *J. Chem. Phys.*, **71** (1979) 1889.
- [10] MATSUO T., *J. Phys. Soc. Jpn.*, **30** (1971) 794.
- [11] MURAKAMI E., KOMUKAE M., OSAKA T. and MAKITO Y., *J. Phys. Soc. Jpn.*, **59** (1990) 1147.
- [12] MATSUO T. and SUGA H., *J. Incl. Phen.*, **2** (1984) 49.
- [13] SIXOU P. and DANSAS P., *Ber. Bunsen Ges.*, **80** (1976) 364.
- [14] SCALAPINO D. J., IMRY Y. and PINCUS P., *Phys. Rev. B*, **11** (1975) 2042.
- [15] HONE D., MONTANO P. A., TONEGAWA T. and IMRY Y., *Adv. Phys.*, **12** (1975) 5141.
- [16] GLAUBER R. J., *J. Math. Phys.*, **4** (1963) 294.
- [17] ZUMER S., *Phys. Rev. B*, **21** (1980) 1298.
- [18] AYTON G., GINGRAS M. J. P. and PATEY G. N., *Adv. Phys.*, **75** (1995) 2360.